Available online at www.sciencedirect.com

ScienceDirect

www.elsevier.com/locate/jes

JES JOURNAL OF ENVIRONMENTAL SCIENCES

www.jesc.cn

Advanced treatment of municipal wastewater by nanofiltration: Operational optimization and membrane fouling analysis

Kun Li[1,2], *Jianxing Wang*[1,2], *Jibao Liu*[1,2], *Yuansong Wei*[1,2,*], *Meixue Chen*[1,2,*]

1. *State Key Joint Laboratory of Environmental Simulation and Pollution Control, Research Center for Eco-Environmental Sciences, Chinese Academy of Sciences, Beijing 100085, China. E-mail: leequeue@hotmail.com*
2. *University of Chinese Academy of Sciences, Beijing 100049, China*

ARTICLE INFO

Article history:
Received 9 June 2015
Revised 10 September 2015
Accepted 11 September 2015
Available online 2 December 2015

Keywords:
Nanofiltration
Municipal wastewater reclamation
Parameters optimization
Membrane fouling
Fluorescence spectral analysis
FT-IR analysis

ABSTRACT

Municipal sewage from an oxidation ditch was treated for reuse by nanofiltration (NF) in this study. The NF performance was optimized, and its fouling characteristics after different operational durations (*i.e.*, 48 and 169 hr) were analyzed to investigate the applicability of nanofiltration for water reuse. The optimum performance was achieved when transmembrane pressure = 12 bar, pH = 4 and flow rate = 8 L/min using a GE membrane. The permeate water quality could satisfy the requirements of water reclamation for different uses and local standards for water reuse in Beijing. Flux decline in the fouling experiments could be divided into a rapid flux decline and a quasi-steady state. The boundary flux theory was used to predict the evolution of permeate flux. The expected operational duration based on the 169-hr experiment was 392.6 hr which is 175% longer than that of the 48-hr one. High molecular weight (MW) protein-like substances were suggested to be the dominant foulants after an extended period based on the MW distribution and the fluorescence characteristics. The analyses of infrared spectra and extracellular polymeric substances revealed that the roles of both humic- and polysaccharide-like substances were diminished, while that of protein-like substances were strengthened in the contribution of membrane fouling with time prolonged. Inorganic salts were found to have marginally influence on membrane fouling. Additionally, alkali washing was more efficient at removing organic foulants in the long term, and a combination of water flushing and alkali washing was appropriate for NF fouling control in municipal sewage treatment.

Introduction

Water crisis has become a prominent issue in China after years of rapid social-economic growth (Jin et al., 2014; Yi et al., 2011). The reclamation of municipal wastewater has been widely recognized as a promising solution to overcome the growing pressure on water resources (Wintgens et al., 2005). Taking Beijing as an example, the reclaimed wastewater utilized in 2013 was 0.8 billion m^3, accounting for 22% of the total water resource demand. The local government has undertaken a series of measures, *e.g.*, Three-year Action Plan to Accelerate the Construction of Wastewater Treatment (2013–2015) and Water Recycling Facilities and Regulations for Wastewater Discharge and Water Reuse (No. 215 Order of

* *Corresponding authors.* E-mails: yswei@rcees.ac.cn (Yuansong Wei), mxchen@rcees.ac.cn (Meixue Chen).

http://dx.doi.org/10.1016/j.jes.2015.09.007
1001-0742/

Table 1 – Characteristics of effluent from oxidation ditch.

Parameter	Average ± S.D.	Parameter	Average ± S.D.	Parameter	Average ± S.D.
pH	7.85 ± 0.064	EC (μs/cm)	787.47 ± 38.35	Cl^- (mg/L)	110.94 ± 0.31
TOC (mg/L)	6.55 ± 0.94	TDS (mg/L)	393.66 ± 19.11	PO_4^{3-} (mg/L)	0.151 ± 0.11
COD (mg/L)	48.70 ± 4.75	Salinity (psu)	0.38 ± 0.03	SO_4^{2-} (mg/L)	59.00 ± 1.60
BOD (mg/L)	7.11 ± 1.84	Alkalinity (mmol/L)	0.49 ± 0.0058	NO_2^- (mg/L)	0.25 ± 0.05
UV_{254} (cm^{-1})	0.154 ± 0.028	K^+ (mg/L)	16.45 ± 0.63	NO_3^- (mg/L)	22.94 ± 0.22
Turbidity (NTU)	0.59 ± 0.070	Ca^{2+} (mg/L)	70.20 ± 0.84	NH_4^+-N (mg/L)	2.39 ± 0.08
Suspended solids (mg/L)	2.52 ± 0.86	Na^+ (mg/L)	84.58 ± 0.38	TN (mg/L)	27.38 ± 3.33
Color (PCU)	72.22 ± 1.92	Mg^{2+} (mg/L)	23.21 ± 0.04	TP (mg/L)	0.500 ± 0.01

the People's Government of Beijing Municipality), to promote and spread utilization of reclaimed wastewater, especially high quality reclaimed water for landscape, greening and industrial uses. The reclaimed wastewater used in 2015 should meet the target of 1 billion m^3 according to the 12th Five-Year Plan (2011–2015) of Beijing (Li et al., 2014). According to the Water Pollution Control Action Plan issued on 2 April 2015 by the State Council of China, the reuse rate of wastewater must be increased to 30% by 2020 in the Beijing–Tianjin–Hebei region. These above mentioned measures and action plans are becoming a strong driving force for spreading wastewater reuse in Beijing.

However, effluents from the existing conventional biological processes of municipal sewage treatment plants could rarely meet the increasingly stringent discharge standards or even standards for water reuse (Jin et al., 2014). Therefore, to satisfy the broad demands for high quality reclaimed water, further advanced treatment technologies, such as membrane technology, are desperately needed. Membrane processes, such as ultrafiltration (UF), nanofiltration (NF) and reverse osmosis (RO), have been widely applied in wastewater treatment and reuse (Jacob et al., 2010; Lau and Ismail, 2009). The UF process could not meet with the requirements for chemical oxygen demand (COD), nitrogen and phosphorus in the new Discharge Standard of Pollutants for Municipal Wastewater Treatment Plant in Beijing (DB11/890-2012), whose requirements are similar to those of the surface water Class IV standard (GB 3838-2002) (except the limit for total nitrogen). It is well known that NF can effectively remove multivalent ions and high molecular weight organic compounds with lower operating pressure and higher permeate flux in comparison with RO. Thus, NF is a promising technology for advanced wastewater treatment considering its energy requirements and cost effectiveness, particularly when both NF and RO are suitable for wastewater reclamation (Alzahrani et al., 2013; Shahmansouri and Bellona, 2015). Despite these advantages, membrane fouling is still a key issue that hinders the application of membrane technologies. The characteristics of wastewater, the operating parameters and the membrane properties all significantly influence the NF performance and its membrane fouling condition. Although many studies have been conducted for the understanding of membrane fouling, the complexity and heterogeneity of foulants in municipal sewage make it difficult to explain the fouling mechanisms. Her et al. (2007) identified that protein- and polysaccharide-like substances were the main foulants, whereas humic substances were not. Chon et al. (2012b) found that major foulants were polysaccharide- and protein-like functional groups produced during biological processes, while inorganic scaling was caused by aluminum, calcium, and silica. Acero et al. (2010) found that membranes with high molecular weight cut off (MWCO) would cause higher fouling resistances, and the external fouling could be pronounced by the increase of transmembrane pressures

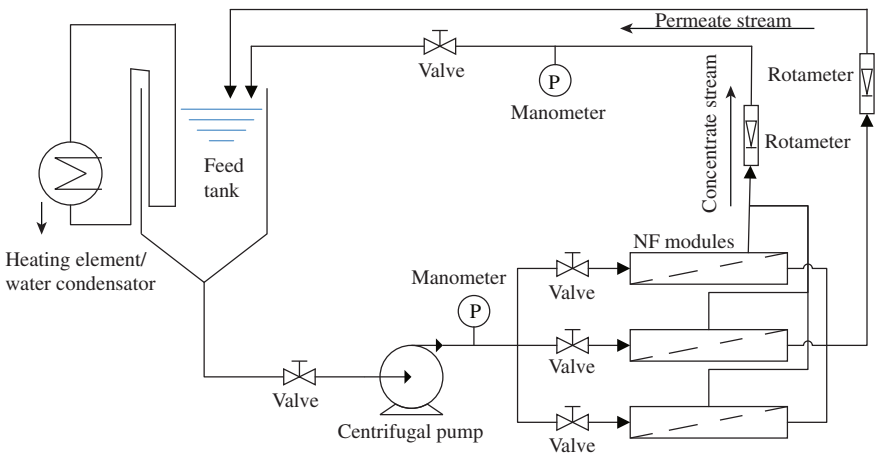

Fig. 1 – Schematic of the nanofiltration (NF) experimental system.

Table 2 – Results of the uniform design experiments.

No. of test	T (°C)	TMP (bar)	pH	Flow rate (L/min)	Membrane	J (L/(hr m^2))	A (L/(hr m^2·bar))
1	(1) 25.0	(4) 6.0	(7) 5.0	(11) 10.0	(13) SD	27.88	4.65
2	(2) 25.0	(8) 8.0	(14) 7.0	(7) 8.0	(11) SD	36.59	4.57
3	(3) 25.0	(12) 10.0	(6) 4.0	(3) 4.0	(9) SP	42.17	4.22
4	(4) 27.5	(1) 4.0	(13) 7.0	(14) 12.0	(7) SP	24.09	6.02
5	(5) 27.5	(5) 6.0	(5) 4.0	(10) 10.0	(5) GE	42.53	7.09
6	(6) 27.5	(9) 8.0	(12) 6.0	(6) 6.0	(3) GE	57.46	7.18
7	(7) 30.0	(13) 12.0	(4) 4.0	(2) 4.0	(1) GE	95.17	7.93
8	(8) 30.0	(2) 4.0	(11) 6.0	(13) 12.0	(14) SD	22.57	5.64
9	(9) 30.0	(6) 6.0	(3) 3.0	(9) 8.0	(12) SD	26.68	4.45
10	(10) 32.5	(10) 10.0	(10) 6.0	(5) 6.0	(10) SP	54.51	5.45
11	(11) 32.5	(14) 12.0	(2) 3.0	(1) 4.0	(8) SP	45.20	3.77
12	(12) 32.5	(3) 4.0	(9) 5.0	(12) 10.0	(6) SP	28.14	2.34
13	(13) 35.0	(7) 8.0	(1) 3.0	(8) 8.0	(4) GE	70.17	8.77
14	(14) 35.0	(11) 10.0	(8) 5.0	(4) 6.0	(2) GE	91.63	9.16
15	(15) 35.0	(15) 12.0	(15) 7.0	(15) 12.0	(15) SD	73.25	6.10

T: temperature, TMP: transmembrane pressure, J: permeate flux; A: permeability, TOC: total organic carbon, EC: electrical conductivity.

(TMP). Antony et al. (2012) suggested that the dominant foulants in RO operation appeared to be humic and neutral fractions. As no consistent conclusions have drawn yet, it is suggested that the knowledge on the development of NF membrane fouling during advanced treatment of municipal sewage with regard to operational duration remains incomplete. In this study, the NF membrane was used to treat effluent of an oxidation ditch from a municipal wastewater treatment plant in Beijing in order to investigate the feasibility of NF membrane application in the reclamation of municipal sewage according to Discharge Standard of Pollutants for Municipal Wastewater Treatment Plant in Beijing (DB11/890-2012). Meanwhile, water qualities of the effluent from the oxidation ditch, the UF process followed the oxidation ditch and the NF permeate was compared with the national discharge standards and standards for water reuse. Moreover, the NF membrane fouling characteristics after different operational durations were also analyzed so as to obtain a comprehensive understanding on the evolution of foulants' contribution over time and then develop corresponding cleaning strategies for the effective control of membrane fouling.

1. Materials and methods

1.1. Wastewater characteristics

The feed water of a laboratory-scale NF membrane setup was the effluent of an oxidation ditch from a municipal wastewater treatment plant with the design capacity of 54,000 m^3/day in Changping District of Beijing, China. The characteristics of the secondary effluent from the oxidation ditch are listed in Table 1. The COD of the secondary effluent was 50 mg/L which barely reached the Class 1A level (*i.e.*, COD ≤ 50 mg/L) of discharge standards. Color was another parameter that could not meet the Class 1A level. Moreover, inorganic ions, such as Cl^-, Na^+, Ca^{2+} and SO_4^{2-}, were also presented in significant amounts.

1.2. Experimental setup and NF membranes

A laboratory-scale NF system (Shanghai Shiyuan Bioengineering Equipment Co., China) shown in Fig. 1 was used in this study, as described by Wang et al. (2013). The system consists of three spiral wound NF modules connected with a centrifugal pump (MG80B2-19FT100-D1, GRUNDFOS, Denmark). The temperature of the feed water was maintained by a heating element and a water condensator. Membrane elements of 1812 size standard from Synder Filtration (SD), GE Water and Process Technologies (GE) and Sepro Membranes (SP) were used, and their characteristics are shown in Appendix A Table S1. NF membranes were chemically cleaned before use to remove pollutants on the membranes. Then the NF membranes were firstly soaked for 12 hr in deionized water and then pressurized under 12 bar for at least 1 hr by deionized water to ensure a steady structure before each experiment. The pure water permeate flux (J_w) was measured at different TMPs before and after each experiment, then the normalized flux (J/J_0) and permeability coefficient (L_p) were calculated to appraise the membrane performance and the extent of membrane fouling. After adjust the pH of feed water using 1 mol/L HCl and 1 mol/L NaOH solutions, the effluent was filtered through a 5-μm security filter. The NF system was operated in a full recycle mode, which meant that both the permeate and the concentrate were recycled back to the feed tank. The permeability of the used membrane was recovered by a cleaning strategy in sequence of water flushing, alkali washing and acid washing after each experiment.

The permeate flux is described by Darcy's law (Eq. (1)):

$$J = \frac{1}{A}\frac{dV}{dt} \tag{1}$$

where J (L/(hr·m^2)) is the permeate flux; A (m^2) is the effective membrane area; V (L) is the total volume of permeate; and t (hr) is the filtration time.

Removal rate (%)													
TOC (mg/L)	UV_{254} (cm^{-1})	EC (mg/L)	Turbidity (NTU)	Color (PCU)	K^+ (mg/L)	Ca^{2+} (mg/L)	Na^+ (mg/L)	Mg^{2+} (mg/L)	Cl^- (mg/L)	NO_2^- (mg/L)	NO^-_3 (mg/L)	PO_4^{3-} (mg/L)	SO_4^{2-} (mg/L)
89.58	94.94	55.31	73.33	100	41.97	94.89	47.08	98.78	36.95	70.41	97.22	80.42	94.39
91.30	97.75	47.65	84.38	100	18.03	74.38	26.05	90.08	28.48	0	66.24	100	85.49
61.08	59.55	19.27	76.67	87.5	5.42	37.05	20.61	50.59	6.91	52.86	93.80	0	61.07
66.66	60.67	11.33	65.63	75	15.19	21.71	17.42	22.82	19.99	0	46.61	100	62.48
87.63	95.51	72.51	84.38	100	59.90	100	64.32	100	67.78	49.17	74.49	100	94.39
64.09	98.31	50.54	84.38	100	26.16	85.76	18.93	96.91	28.27	0	59.06	100	100
86.53	100	65.35	80.65	100	87.54	100	44.01	98.78	58.50	13.59	61.71	100	98.41
91.99	96.63	36.70	86.84	100	6.45	84.49	4.41	95.83	17.61	36.00	29.16	100	94.05
86.50	94.12	11.85	90.57	100	80.41	100	86.12	100	56.77	0	31.25	60.07	87.98
62.95	66.11	8.025	88.52	87.5	24.82	15.39	9.05	13.67	3.96	0	2.01	31.44	72.65
78.13	64.29	2.42	88.89	83.33	59.96	65.30	30.63	77.78	26.23	100	7.67	17.92	49.98
60.05	58.79	10.86	82.69	71.43	10.76	25.72	5.68	28.17	5.64	0	2.77	21.12	53.60
83.44	96.10	47.76	86.84	100	82.26	100	82.44	98.80	69.42	0	67.59	38.08	80.85
69.77	91.67	69.64	88.57	100	42.14	97.96	40.77	98.13	64.84	0	50.41	85.43	96.55
100	97.04	49.42	75	100	50.56	95.44	29.81	81.93	42.93	67.91	11.69	92.48	81.31

The permeability is calculated by the following formula (Eq. (2)):

$$L_p = \frac{J}{\Delta P_{TM} - \Delta\pi} \tag{2}$$

where L_p (L/(hr·m^2·bar)) is the permeability and ΔP_{TM} (bar) is the TMP; and $\Delta\pi$ (bar) is the osmotic pressure difference over the membrane.

The boundary flux theory (Stoller and Ochando-Pulido, 2014, 2015) was introduced to predict the evolution of permeate flux in the long run. The fitted flux was calculated using Eqs. (3) and (4):

$$J_p(t) = J_{p,0} - a \cdot t; \qquad J_p(t) < J_b \tag{3}$$

$$J_p(t) = (J_{p,0} - J_b) \cdot e^{b \cdot t} + J_b - a \cdot t; \qquad J_p(t) \geq J_b \tag{4}$$

where $J_p(t)$ (L/(hr·m^2)), $J_{p,0}$ (L/(hr·m^2)) and J_b (L/(hr·m^2)) are the permeate flux at a given time, the initial permeate flux and the boundary permeate flux, respectively, whereas a and b are fouling fitting parameters.

$$m(t) = \frac{J_p(t)}{P_{TM}(t)} \tag{5}$$

$$\frac{\Delta m}{\Delta t} = \frac{J_p(t_2)}{P_{TM}(t_2)} - \frac{J_p(t_1)}{P_{TM}(t_1)} \tag{6}$$

where $m(t)$ is the permeability at a given time t, and $\Delta m/\Delta t$ was calculated between two points at times t_1 and t_2 during the operational duration to predict the variation trend of permeate flux.

The total filtration resistance (R_t) was calculated using Eq. (7):

$$R_t = \frac{TMP}{\mu J} \tag{7}$$

where R_t (m^{-1}) is the filtration resistance; TMP (bar) is the transmembrane pressure; J ($m^3/(m^2 \cdot sec)$) is the permeate flux; and μ (bar·sec) is the permeate viscosity.

The rejection rates of NF were calculated using Eqs. (8) and (9):

$$R_{tot} = 1 - \frac{C_p}{C_{bi}} \times 100\% \tag{8}$$

$$R_{obs} = 1 - \frac{C_p}{C_b} \times 100\% \tag{9}$$

where R_{tot} and R_{obs} are the total rejection rate and the observed rejection rate, respectively; C_p, C_{bi} and C_b describe the solute concentrations in the permeate, the initial bulk solution and the bulk solution, respectively, mg/L.

1.3. Optimization of NF membrane performance

The optimization of NF membrane performance in municipal sewage treatment consists of two parts: the selection of membranes and the optimization of operating parameters. Two groups of experiments were performed to achieve the goals. The selection of membranes was arranged according to a uniform design of experiments. The statistical experiment method developed by Fang and Wang (1993) can replace the complete combination of experimental parameters by using relatively fewer experiment trials uniformly distributed within the parameter space (Li et al., 2003). The effects of temperature, TMP, pH, feed flow rate and membrane type were examined. There were 3-5 levels for the experimental factors and a U_{15} ($5^4 \times 3^1$) mixed-level uniform design was selected. The factors and levels of these tests are listed in Appendix A Table S2. Then, further optimization of the NF parameters was carried out using a L_9 (3^4) orthogonal experimental design (Appendix A Table S3).

1.4. Membrane fouling experiments

The membrane fouling experiments were operated under the optimized parameters with different operational durations

(*i.e.*, 48 and 169 hr). The operational conditions were monitored, and samples of the feed, NF concentrate and NF permeate were taken for further analysis at given intervals. The membrane used was recovered by cleaning with water flushing, alkali washing and acid washing after each experiment, and samples of the cleaning water in each step were analyzed to investigate the conditions of membrane fouling.

1.5. Analytical methods

Water parameters such as NH_4^+-N, TN and total phosphorus (TP), were determined according to Standard Methods (Federation and Association, 2005). The concentration of COD was measured by a DR2800 spectrophotometer (HACH, USA). Total organic carbon (TOC) was determined by a TOC-VCPH analyzer (Shimadzu, Japan). UV_{254} was measured by an ultraviolet and visible spectrophotometer (Spectrum Lab 752sp, Lengquang Tech., China). Conductivity was measured with a conductivity meter (HI4321, Hanna, Italy).

The contents of Na^+, K^+, Ca^{2+} and Mg^{2+} were analyzed by an inductively coupled plasma-optical emission spectroscopy (Optima 2100 DV, Perkin Elmer, USA). The amounts of anions (*i.e.*, Cl^-, NO_3^-, NO_2^-, SO_4^{2-} and PO_4^{3-}) were determined using an ion chromatography (ICS-1000, Dionex, USA). A turbidity meter (Turb 550, WTW, Germany) was used to measure turbidity.

A fluorescence spectrophotometer (F-7000, Hitachi, Japan) and a gel permeation chromatography-UV detector (GPC) with a high performance liquid chromatography (HPLC) system (Breeze 1525, Waters Co, USA) were used to investigate the major components and the complexity of organic matters in water samples. A Fourier transform infrared spectrometer (FT-IR, Nicolet 8700, Thermo Electron Corporation, USA) with a resolution of 4 cm^{-1} within 400–4000 cm^{-1} was used to obtain information about the functional groups of organic matters presented in freeze-dried samples including the feed, concentrate and permeate of the NF process and the cleaning water samples from water flushing, alkali washing and acid washing. The amounts of polysaccharides and proteins in EPS were measured by colorimetric methods (Dubois et al., 1956; Lowry et al., 1951).

1.6. Statistical analysis

All the experimental data were analyzed using SPSS version 18.0 software for one-way analysis of variance (ANOVA). The relationships between operating parameters and membrane performance were analyzed by Pearson analysis, and P-values less than 0.05 were considered to indicate statistically significant differences.

2. Results and discussion

2.1. Selection of NF membranes and optimization of operational parameters

To get an optimized performance of NF in municipal sewage treatment, the selection of membranes was carried out through a uniform design of experiments (Table 2), and the operational parameters were further optimized through a group of orthogonal design experiments (Table 3).

The permeate flux (J), as one of the most important factors indicating the performance of membrane process, reached the maximum of 95.17 L/(hr·m^2) in Test 7 listed in Table 2 (T = 30.0°C, TMP = 12.0 bar, pH = 4.0, flow rate = 4.0 L/min, GE membrane). According to the Pearson correlation analysis summarized in Appendix A Table S4, the selection of membrane was significantly and positively correlated with permeate flux (J), permeability (A) and the removal rate of electrical conductivity (R_{EC}), while the GE membrane was selected because of its relatively higher J, A and R_{EC} in comparison with the other two membranes based on the data summarized in Table 2. Furthermore, other parameters, namely TMP, flow rate and pH, also showed significantly correlations with various removal rates, and were further optimized through a group of orthogonal design experiments (Table 3). Temperature was found significantly related to J, R_{TOC} and R_{EC}, then the energy consumption for heating and the water used for cooling of the NF system turned into the key factors that decided the selection of temperature. The heat generated by the high pressure pump of the NF system during a long operational duration make it unstable keep the feed at ambient temperature, and it was found that the water use of the cooling system was minimized at 30°C, while more water was needed for cooling to keep a temperature lower than 30°C and more energy would be consumed for heating to keep a temperature higher than 30°C. Thus, the temperature was set at 30°C for convenience.

The ANOVA was performed to determine the influence and relative importance of the factors (Gönder et al., 2010). Results showed that the TMP had significant correlations with J and the removal rate of TOC, whereas the pH and flow rate had no significant relationship with the membrane performance. Combined with the intuitionistic analysis (Appendix A Table S5), a comprehensive optimum scheme was achieved at TMP = 12 bar, pH = 4 and flow rate = 8 L/min.

The membrane performance of nanofiltration under optimized parameters was verified and the permeate water quality was compared with the effluent water quality from the oxidation ditch process, the UF process of the treatment station and the standards of reclaimed water quality for different uses (Li et al., 2014) (Table 4).

The NF permeate could fully meet with the requirements of water reclamation for different uses, whereas the effluent from the oxidation ditch or UF process could only meet with most limitations in Class 1A except for color. Furthermore, both the effluent from the oxidation ditch and the UF process could not meet the surface water Class IV standard or the local standards for water reuse in Beijing (DB11/890-2012). It is striking to note that the UF process after oxidation ditch only marginally improved the water quality, whereas the NF process showed a significant improvement in water quality.

2.2. Membrane fouling of NF with different operational durations

2.2.1. Permeate flux

The evolution of the permeate flux decline at different operational durations could be divided into two stages

Table 3 – Results of the orthogonal design experiments.

Item	TMP	pH	Flow rate	Error	J	A	Removal rate (%)											
	A	B	C	D			TOC	UV_{254}	EC	Turbidity	Color	K^+	Ca^{2+}	Na^+	Mg^{2+}	Cl^-	NO_2^-	NO_3^-	PO_4^{3-}	SO_4^{2-}
1	(1) 8	(1) 4.0	(1) 6	1	68.01	8.52	67.09	94.85	49.48	88.09	100	93.71	100	85.47	100	66.19	73.52	43.94	49.46	100
2	(1) 8	(2) 5.0	(2) 8	2	70.25	8.76	77.45	95.94	67.71	78.57	100	43.54	100	36.24	100	66.21	40.47	43.5	83.82	100
3	(1) 8	(3) 6.0	(3) 10	3	70.4	8.79	81.93	94.07	52.64	72.72	100	21.89	88.57	15.76	94.03	49.43	50.79	26.98	100	100
4	(2) 10	(1) 4.0	(2) 8	3	88.97	8.88	79.02	97.01	74.11	80	100	61.37	100	52.62	100	74.29	61.29	47.88	64.49	100
5	(2) 10	(2) 5.0	(3) 10	1	86.89	8.64	83.64	97.03	59	58.82	100	26.19	98.71	20.21	96.59	56.92	50.79	34.17	100	100
6	(2) 10	(3) 6.0	(1) 6	2	85.14	8.49	100	97.87	54.04	76.19	100	24.77	88.06	19.22	93.63	52.36	45.78	30.41	100	100
7	(3) 12	(1) 4.0	(3) 10	2	102.78	8.55	100	98.49	76.95	82.75	100	56.34	100	56.49	98.11	76.15	38.7	56.86	100	88.8
8	(3) 12	(2) 5.0	(1) 6	3	101.07	8.44	100	99.24	61.63	83.33	100	28.95	100	22.97	99.67	61.46	50.06	40.55	100	100
9	(3) 12	(3) 6.0	(2) 8	1	101.52	8.46	100	100	55.85	76.67	100	28.04	88.97	19.61	94.58	55.2	45.47	33.25	100	100

(Acero et al., 2010; Ochando-Pulido et al., 2014; Stoller and Ochando-Pulido, 2015). A rapid decline of permeate flux was observed initially, and the flux decline rates during the first 8 hr of operation were found to be nearly identical in both experiments which could be defined as the first stage. Then, the flux decline rate gradually decreased and enters a steady state in the second stage, indicating that the NF process approached a quasi-steady state. The proportions of flux decline at different operational durations, 5.79% and 6.44% for the 48-hr and 169-hr experiments, respectively, showed no significant differences, indicating a relatively slower fouling state achieved in the second stage (Fig. 2a and b).

To predict the decline of permeate flux in the long run and optimize the frequency of membrane cleaning, a series of equations were conducted to modelize the flux behavior of the membranes as a function of the operation time. The theories of critical and threshold flux were used as important tools to optimize the performance of NF membrane systems, while there were still some limits that cannot satisfy the need of the operational conditions. Previous publications (Ochando-Pulido et al., 2014; Stoller and Ochando-Pulido, 2014, 2015) merged those two theories into a new concept called boundary flux, which was adapted to the modelization of NF membrane system in the tertiary treatment of the effluents from olive oil mills. The experimental data fitted the boundary flux equations well and it was found to be an effective way to improve the operating strategy and prolong the operating duration of NF membrane system.

The experimental data was fitted by Eq. (4) based on the boundary flux theory, and the results are shown in Fig. 3 and Table 5. Similarly, the trend of $\Delta m/\Delta t$ in these two experiments also support the two stage theory mentioned above, and the values hardly changed after a first few hours of operation which indicated that the permeate flux would decline in a linear fashion in the long run. It was found that Eq. (4) fit the two experiments well ($R^2 > 0.92$), which indicated that the operational conditions could be further optimized to get a more sustainable permeate flux with a lower cost. The first term of Eq. (4) would become ignorable with time prolonged, then the Eq. (4) was simplified and turned into a linear relationship similar to Eq. (5). The NF membrane needs cleaning when the normalized permeate flux declined by 10% according to the operating manuals from manufacturers, thus the operational duration could be calculated by the simplified Eq. (4) (results listed in Table 5). Furthermore, it was interesting to observe that a much longer expected operational duration was achieved on the basis of the longer duration experiment (175% longer than the shorter one), which suggested that the operational condition control needs to be more precise and the fitting equation might also need a further optimization. The decline of permeate flux was a consequence of membrane fouling due to several causes, such as the formation of cake layer, pore blocking, or the adsorption of solutes onto the membrane.

2.2.2. Rejection rate of organic and inorganic components

The TOC rejection rate exhibited a waving increase, and the trends of R_{tot} and R_{obs} were roughly the same in the 48-hr

Table 4 – Comparison of water qualities and standards.

Water quality	COD (mg/L)	BOD (mg/L)	TOC (mg/L)	UV_{254} (cm^{-1})	EC (mg/L)	TDS (mg/L)	Salinity (psu)	Total hardness ($CaCO_3$ mg/L)	Alkalinity ($CaCO_3$ mg/L)
Effluent from oxidation ditch	48.70	7.11	6.55	0.154	787.47	393.66	0.38	272.26	233.5
UF permeate	25.56	3.45	3.51	0.145	764.58	382.29	0.37	272.03	
NF permeate	N.D[a]	N.D	0.38	0.006	345.1	172.5	0.16	1.975	
Water standard									
First grade A[b]	50	10	–	–	–	–	–	–	–
Class 1B[b]	60	20	–	–	–	–	–	–	–
Surface water Class IV	≤30	≤6	–	–	–	–	–	–	–
Reclaimed for urban uses	–	–	–	–	–	≤1000/1500	–	–	–
Reclaimed for scenic environment	≤30/40	–	–	–	–	–	–	–	–
Reclaimed for industrial uses	≤60	–	–	–	–	≤1000	–	≤450	≤350
Reclaimed for groundwater recharge	≤15/40	–	–	–	–	≤1000	–	≤450	–
Reclaimed for farmland irrigation	≤100/200	–	–	–	–	≤1000/2000	–	≤450	–

a N.D, not detected.
b Class 1A and B in "Discharge standard of pollutants for municipal wastewater treatment plant" (GB18918-2002).
c When water temperature > 12°C use the value out of parentheses, otherwise use the value in parentheses.
d According to the requirements of reclaimed water quality in Beijing, the reclaimed water quality was upgraded from Class 1B to Surface water Class IV (except the limit for TN).

experiment (Fig. 4). R_{tot} was found higher than R_{obs}, while the TOC concentration in both the feed and NF permeate generally decreased. These results indicated that some organic matters had deposited onto the membrane surfaces or penetrated into its pores. Pore blocking and cake layer formation could be the primary causes for the observed decrease in the permeate flux (Acero et al., 2010; Xu et al., 2010). The trend of TOC during the initial 44 hr of the 169-hr experiment was similar to that observed in the 48-hr experiment; then, R_{obs} grew to exceed R_{tot} after 44 hr, which persisted until the end of the test. Considering the increasing TOC in the feed, it was reasonable to presume that the organic matters deposited onto the membrane began to desorb and release back into the bulk solution. However, no flux recovery was observed with this assumed desorption (Fig. 2b), suggesting that concentration polarization became another key factor of membrane fouling in the second stage. The variations of EC and turbidity showed no significant differences between the two experiments. The increase of salinity in the feed and permeate led to a decreasing trend in both R_{tot} and R_{obs}, which implied that concentration polarization could be more severe with the increase of time. The rapid decrease of R_{obs} in turbidity indicated that the rapid deposition of suspensions and colloid substances on the membrane also contributed to the pore blocking and cake layer formation processes.

2.3. Characterization of NF membrane foulants

2.3.1. Molecular weight distribution and fluorescence spectral analyses

Fig. 5 shows the molecular weight (MW) distribution of the samples in two fouling experiments. Three primary peaks (*i.e.*, 1082, 1190 Da; 2005, 2164 Da; 2988, 3016 Da) were found in the feed and NF concentrate at the end of each experiment, while only two weak peaks with low MW (*i.e.*, 706, 870 Da; 1092, 1179 Da) appeared in the NF permeate. The peak intensity of the NF concentrate in the 48-hr experiment was almost all weaker than that of the feed, however, opposite trend appeared in the 169-hr experiment that the peaks in NF concentrate were significantly stronger than that of the feed. These variations indicated that the organic matters, particularly that with higher MW, deposited onto the membrane and into the pores, which was related to the rapid flux decline at the first stage; then, the deposited organic matters began to desorb and significant concentration polarization was developed which well supported the presumption in Section 2.2.2. Furthermore, significant differences were found between cleaning water samples at different operational durations. The water flushing samples were composed of low MW (*i.e.*, <5000 Da) with high intensity which is typically related to humic substances (Chon et al., 2012a; Her et al., 2007), indicating that the humic substances could be removed easily by physical cleaning. High MW foulants (*i.e.*, 36,612, 39,501 and 41,816 Da) that are typically associated with non-humic substances (Chon et al., 2012a) were primarily contained in alkaline washing samples, while others appeared in acid washing samples. Protein-like substances distributed across low and high MW and were included in the non-humic substances according to former studies (Chon et al., 2012b; Her et al., 2007), implying that protein-like substances contributed to irreversible fouling that could only be removed by chemical cleaning. It is also noteworthy that the alkaline solution became more efficient in organic foulants removal after a longer operational duration, which indicated that the reversible fouling gradually became irreversible with time prolonged. These results suggested that an appropriate cleaning cycle as well as a reasonable selection of cleaning methods are crucial for the membrane fouling control of NF.

Fluorescence excitation–emission matrix (EEM) of the organic matters is shown in Fig. 6 and the peak intensities are summarized in Table 6. The distribution of the peaks was divided into five regions as mentioned elsewhere (Chen et al., 2003). Both the humic-like and protein-like

SS (mg/L)	Turbidity (NTU)	Color (PCU)	K^+ (mg/L)	Na^+ (mg/L)	Ca^{2+} (mg/L)	Mg^{2+} (mg/L)	Cl^- (mg/L)	NO_3^- (mg/L)	NO_2^- (mg/L)	PO_4^{3-} (mg/L)	SO_4^{2-} (mg/L)	NH_4^+–N (mg/L)	TN (mg/L)	TP (mg/L)
2.52	0.63	72.22	16.45	84.58	70.20	23.21	110.94	22.94	0.25	0.151	59.00	2.39	27.38	0.500
1.33	0.56	56.67	16.17	85.17	69.88	23.36	108.43	15.74	0.21	0.148	60.11	1.22	19.29	0.558
N.D	0.04	0	5.82	49.37	0.79	N.D	74.02	7.36	0.002	0.038	N.D	0.56	9.18	0.051
10	–	30	–	–	–	–	–	–	–	–	–	5(8)[c]	–	–
20	–	30	–	–	–	–	–	–	–	–	–	8(15)[c]	–	–
–	–	–	–	–	–	–	≤250	≤10	–		≤250	≤1.5	1.5[d]	≤0.1/0.3
–	≤5/10	≤30	–	–	–	–	–	–	–	–	–	≤10–20	–	–
≤10/20	≤5	≤30	–	–	–	–	–	–	–	–	–	≤5	–	≤0.5/1
≤30	≤5	≤30	–	–	–	–	≤250	–	–	–	≤250/600	≤10	–	≤1
–	≤5/10	≤15/30	–	–	–	–		≤15	≤0.02	–	–	≤0.2/1	–	≤1
≤60/100	≤10	≤30	–	–	–	–	350	–	–	–	–		–	–

substances increased with operational duration in the NF concentrate, whereas the variations were not evident in NF permeate which indicated a stable output water quality. Additionally, only the intensity of Peak A (*i.e.*, aromatic proteins in Region I) was weaker in the NF concentrate, while the other peaks increased due to membrane rejection. This phenomenon implied that the aromatic proteins were easily deposited onto the membrane or into its pores. Significant differences were found in the cleaning water samples between the 48-hr and 169-hr experiments. Weaker peaks appeared in WC samples after longer operational duration, while those in AlkC samples and AcidC samples (except Peak A) were stronger, indicating the increase of adhesion strength between foulants and membrane with time. From the analysis of MW distribution and fluorescence characteristics, it could be asserted that the formation of membrane fouling over the long term operation is closely associated with high MW protein-like substances.

2.3.2. FT-IR analysis

The FT-IR spectra of freeze-dried samples including the feed, concentrate and permeate of the NF process and the cleaning water samples are shown in Fig. 7. Although FT-IR may not be useful in identifying specific compounds of complex components, the major or representative functional groups can be determined through the summation of IR absorbance (or transmittance) of samples.

The peaks in the range of 3500–3300,1490–1440 and 850–750 cm^{-1} could be attributed to N–H stretching and C–N stretching in amides, and the peak in the range of 1680–1630 cm^{-1} was indicative of the carbonyl CO band of primary amides. These amide groups were associated with protein-like substances released by microbial metabolism. The peaks in the range of 3100–2900 cm^{-1} (*i.e.*, O–H stretching) and 1740–1720 cm^{-1} (*i.e.*, carbonyl CO band) were attributed to the carboxylic acids of the humic substances, and the C–H band appeared in the range of 2900–2800 cm^{-1} could be related to aldehydes. The C–O stretching and the O–H band

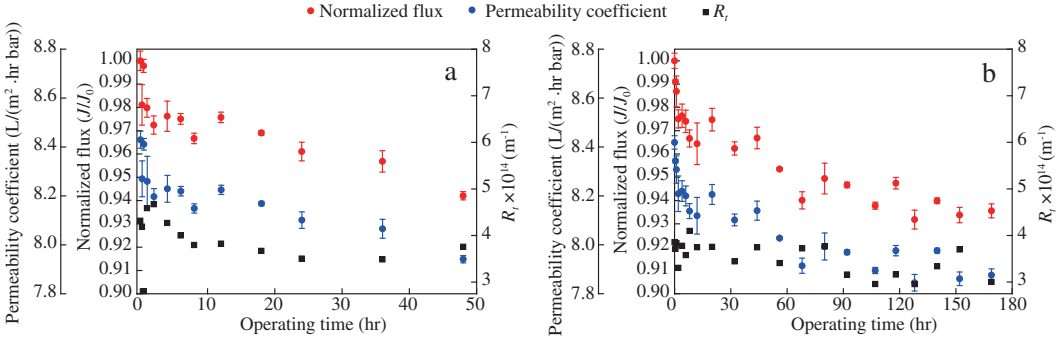

Fig. 2 – Variations of the permeate flux and filtration resistance (R_t) at different operational durations: (a) 48-hr experiment; (b) 169-hr experiment.

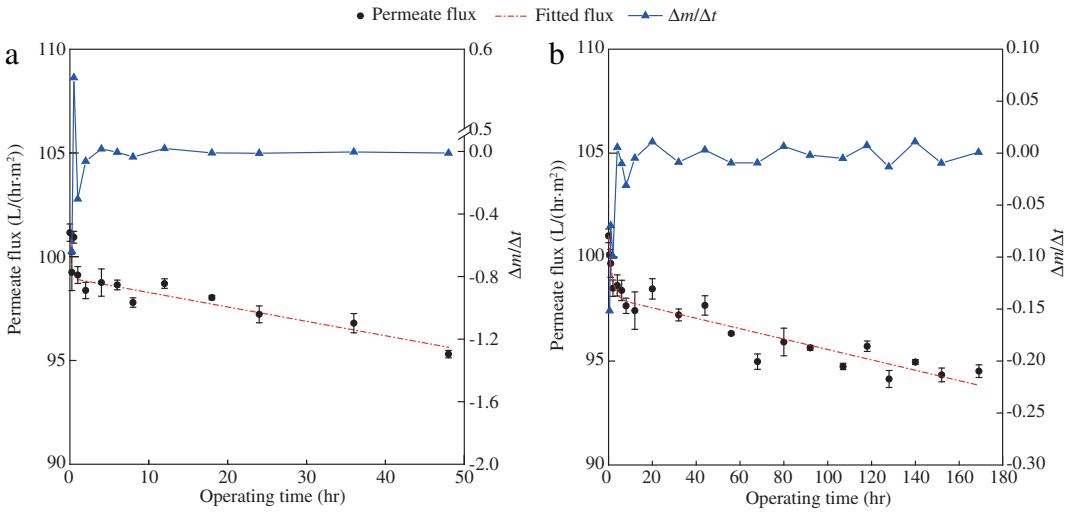

Fig. 3 – Evolutions of NF permeate flux and the fitted flux at different operational durations: (a) 48-hr experiment; (b) 169-hr experiment. NF: nanofiltration.

were detected in the range of 1350–1260 and 1075–1000 cm^{-1}, respectively, which were derived from the polysaccharide-like substances (Chon et al., 2012a, 2012b; Wang et al., 2015). The O–H stretching and C–H stretching that occurred in the range of 3500–3300 and 3000–2800 cm^{-1} were related to proteins, humic acids and polysaccharides, and it was difficult to distinguish the derivation of these functional groups based on IR analysis. The peak intensity in the range of 3500–3300 cm^{-1} in WC samples became weaker as the operational duration increased, while that in AlkC samples increased, indicating that alkali washing was more efficient at removing those three types of organic foulants over the long term. Other peaks (*i.e.*, 1680–1630 cm^{-1}, 1490–1440 cm^{-1}, 1350–1260 cm^{-1} and 1210–1100 cm^{-1}) were found to be significantly weakened in WC samples, suggesting that the roles of both humic and polysaccharide-like substances were diminished, while the role of protein-like substances was strengthened in the contribution of membrane fouling over time.

2.3.3. EPS analysis

The EPS content and its composition were detected and shown in Appendix A Fig. S1. The proportion of proteins in WC samples increased with operational duration while that of polysaccharide decreased, which well supported the conclusion that proteins played a much more important role in the membrane fouling with longer operational duration. Additionally, the protein content in the permeate showed a relative increase while the polysaccharide content decreased, implying that more proteins may have deposited onto the membrane or into its pores which lead to the increase of proteins in the permeate.

2.3.4. Inorganic salts

NaOH and HCl solutions were used for the alkali washing and acid washing, respectively; thus, it was no surprise to find a relatively high content of Na^+ and Cl^- in AlkC and AcidC samples, respectively. Water flushing was found to be the most efficient way for inorganic fouling control (Appendix A Fig. S2), indicating that inorganic salts primarily contributed to the concentration polarization. The concentrations of Ca^{2+} and SO_4^{2-} increased in AlkC samples while no significant variations were found in AcidC samples as a function of operational duration. This phenomenon indicated that calcium sulfate might be formed in the feed side and entrapped by sticky organic fouling layers that could be removed by alkali washing, while very limited amounts of inorganic salts deposited directly onto the membrane surface. Based on these results, inorganic salts in municipal sewage seem to have only a marginal contribution to membrane fouling.

3. Conclusions

The optimization of NF membrane performance in municipal sewage treatment for water reuse and the fouling characteristics after different operational durations were investigated to elucidate a comprehensive understanding

Table 5 – Parameters in the boundary flux equations at different operational durations.

Parameter	48-hr experiment	169-hr experiment
$J_{p,0}$ (L/(hr·m²))	101.15	101.02
a (L/(hr·m²))	0.0694	0.0250
b (hr^{-1})	8.0702	0.6308
J_b (L/(hr·m²))	98.97	98.06
R^2	0.9434	0.9279
Expected operational duration[a] (hr)	142.6	392.6

[a] The expected operational duration was calculated based on the simplified Eq. (4).

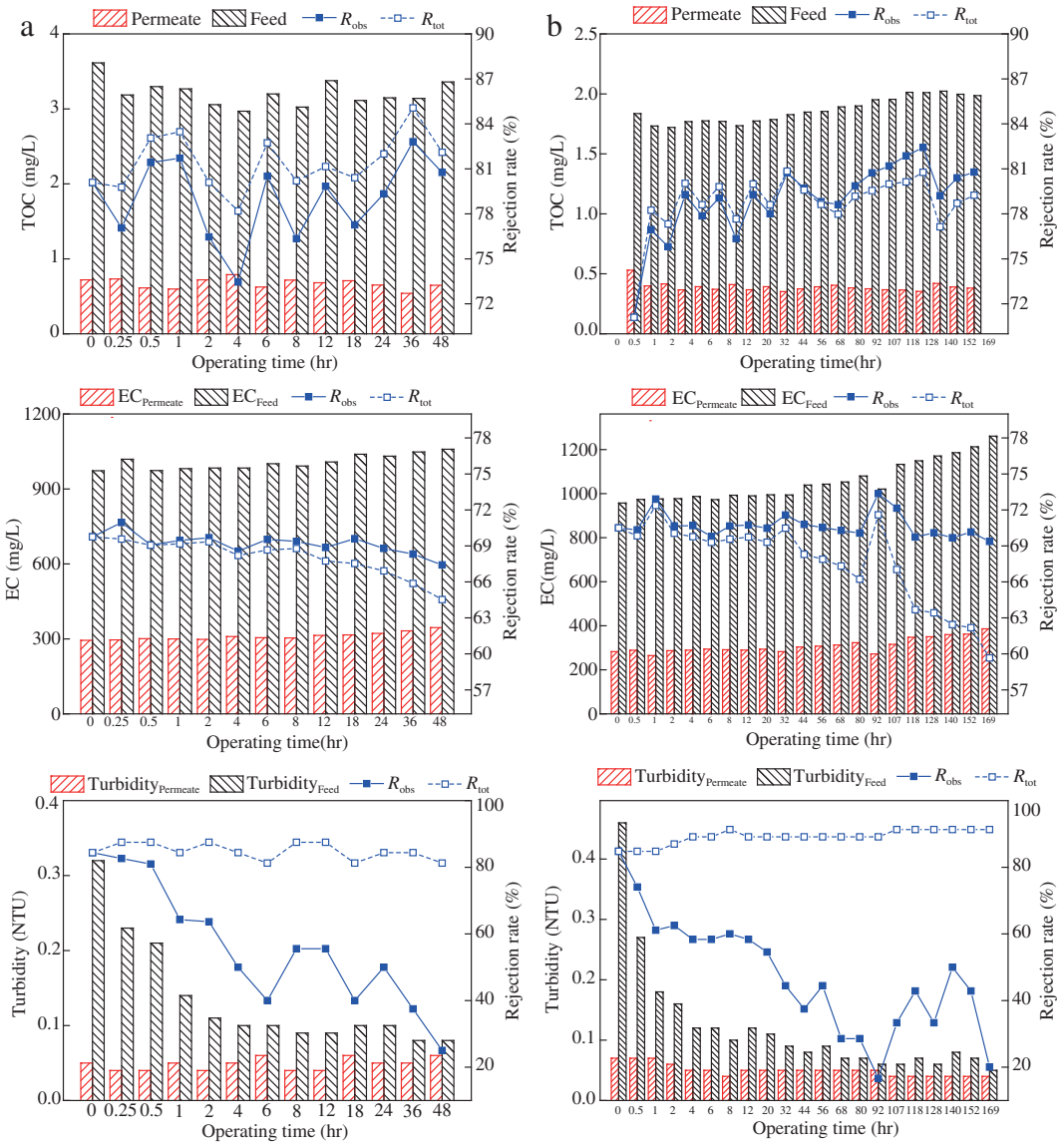

Fig. 4 – Variations of TOC, EC and turbidity at different operational durations: (a) 48-hr experiment; (b) 169-hr experiment.

on the applicability of nanofiltration in the reclamation of municipal sewage. An NF membrane from GE was selected through a U15 ($5^4 \times 3^1$) mixed-level uniform design of experiments, and further optimization of parameters were then determined based on an L9 (3^4) orthogonal experimental design. A comprehensive optimized scheme was achieved at TMP = 12 bar, pH = 4 and flow rate = 8 L/min. The permeate water quality was shown to fully meet with the requirements of water reclamation for different uses and the surface water Class IV standard as well as the local standards for water reuse in Beijing (DB11/890-2012). Results of the membrane fouling experiments after different operational durations (*i.e.*, 48-hr and 169-hr) showed that the flux decline could be divided into two stages: a rapid flux decline in the first 8 hr and then a quasi-steady state with a relatively stable flux. The boundary flux theory was used to predict the evolution of permeate flux, and the results showed that the expected operational duration calculated based on the 169-hr experiment was 392.6 hr which is 2.75 times that of the 48-hr experiment, suggesting the need of further optimization in operational condition control and the fitting equation. From the perspectives of MW distribution and fluorescence characteristics of the cleaning water samples, the formation of membrane fouling is closely associated with high MW protein-like substances over the long term. IR spectra analysis suggested that the roles of both humic and polysaccharide-like substances diminished with operational duration, while the role of protein-like substances strengthened with regard to membrane fouling; these results were also well supported by the variations of the EPS content and its composition. Inorganic salts in municipal sewage were

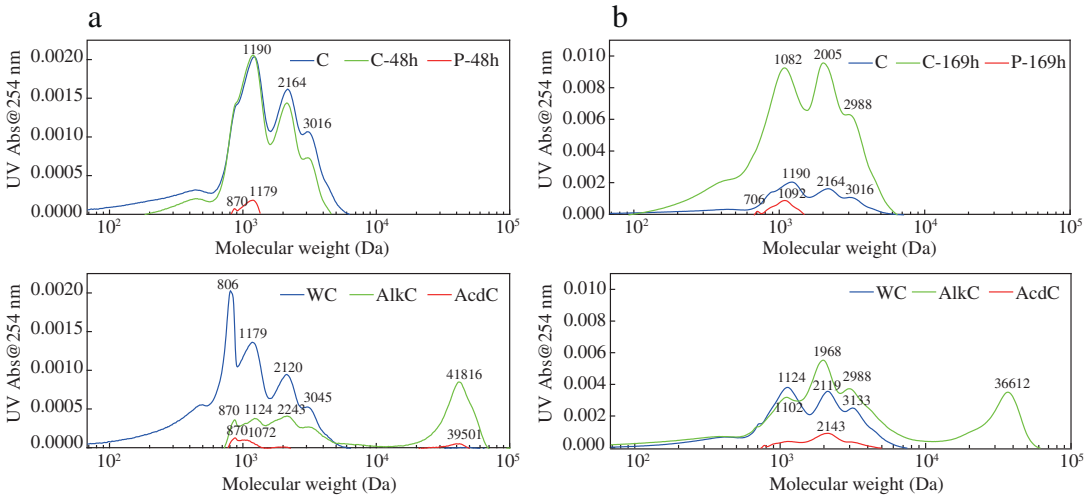

Fig. 5 – Molecular weight (MW) distributions of organic matters in water samples: (a) 48-hr experiment; (b) 169-hr experiment. C-48 hr and C-169 hr: NF concentrate at the end of the 48-hr experiment and the 169-hr experiment, respectively; P-48 hr and P-169 hr: NF permeate at the end of the 48-hr experiment and the 169-hr experiment, respectively; WC: water flushing cleaning; AlkC: alkali washing cleaning; AcidC: acid washing cleaning.

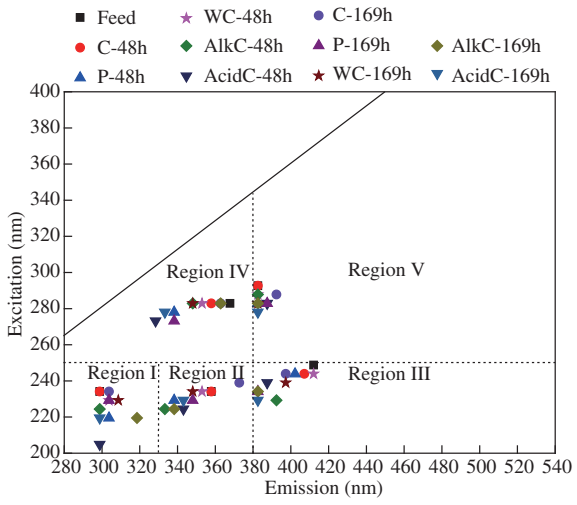

Fig. 6 – Fluorescence excitation–emission matrix (EEM) of the organic matters in water samples. Region I: Aromatic Protein I; Region II: Aromatic Protein II; Region III: Fulvic acid-like substances; Region IV: Soluble microbial by-product-like substances; Region V: Humic acid-like substances.

shown to have only a marginal contribution to membrane fouling. Alkali washing was shown to be more efficient at removing organic foulants over the long term, and a combination of water flushing and alkali washing was suggested to be a better cleaning strategy for NF fouling control of NF in the municipal sewage treatment in the long run.

Acknowledgments

This work was supported by the Major Science & Technology Projects for Water Pollution Control and Management of China (Nos. 2012ZX07203-002; 2015ZX07203-005).

Appendix A. Supplementary data

Supplementary data to this article can be found online at http://dx.doi.org/10.1016/j.jes.2015.09.007.

Table 6 – Peak intensity of fluorescent substances in water samples.

Peak	Feed	C (48 hr/169 hr)		P (48 hr/169 hr)		WC (48 hr/169 hr)		AlkC (48 hr/169 hr)		AcidC (48 hr/169 hr)	
A	333.7	327.3	323.2	134.3	138.6	293.1	297.8	216.8	272.3	362.4	156.3
B	1033	832.3	1012	440.3	448	726.2	685.5	591.9	676.5	508	529.5
C	923.9	879.6	1083	147.3	203.3	561.3	520.5	230.3	502.8	102.8	156.5
D	1013	799.7	982.1	213.5	209.3	582.1	498.8	263.8	429.4	151.8	175.6
E	943.1	761.3	960	126.8	123.1	538.8	432	202	411.1	53.62	83.47
F	–	–	–	–	–	1139	–	–	–	–	–

A: Tyrosine & protein-like substances (Region I); B: Protein-like substances (Region II); C: Hydrophobic acid, fulvic acid (Region III); D: Tryptophan and protein-like substances related to the biological process (Region IV); E: Marine humic acids, humic acid-like substances (Region V); F: humic acid-like substances (Region V).

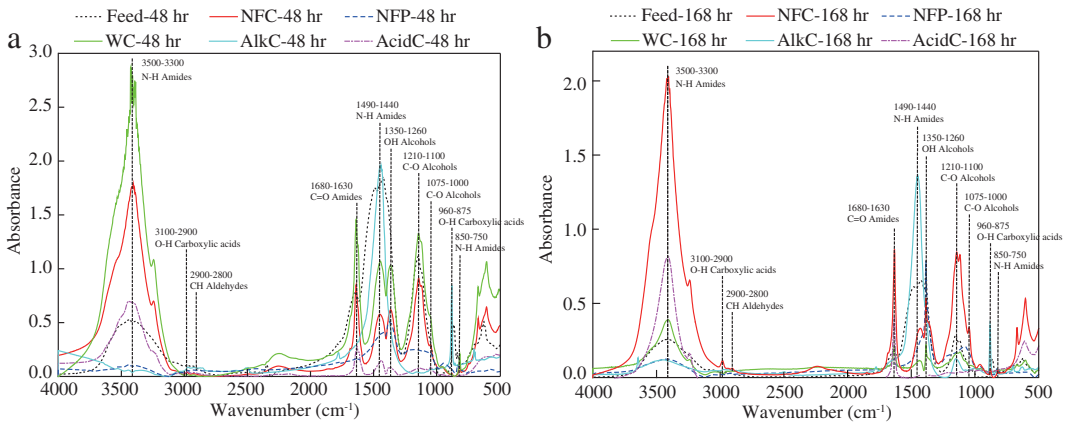

Fig. 7 – Infrared radiation (IR) spectra of organic matters in water samples: (a) 48-hr experiment; (b) 169-hr experiment.

REFERENCES

Acero, J.L., Benitez, F.J., Leal, A.I., Real, F.J., Teva, F., 2010. Membrane filtration technologies applied to municipal secondary effluents for potential reuse. J. Hazard. Mater. 177 (1), 390–398.

Alzahrani, S., Mohammad, A., Hilal, N., Abdullah, P., Jaafar, O., 2013. Comparative study of NF and RO membranes in the treatment of produced water—part I: assessing water quality. Desalination 315, 18–26.

Antony, A., Subhi, N., Henderson, R.K., Khan, S.J., Stuetz, R.M., Le-Clech, P., et al., 2012. Comparison of reverse osmosis membrane fouling profiles from Australian water recycling plants. J. Membr. Sci. 407, 8–16.

Chen, W., Westerhoff, P., Leenheer, J.A., Booksh, K., 2003. Fluorescence excitation-emission matrix regional integration to quantify spectra for dissolved organic matter. Environ. Sci. Technol. 37 (24), 5701–5710.

Chon, K., Cho, J., Shon, H.K., Chon, K., 2012a. Advanced characterization of organic foulants of ultrafiltration and reverse osmosis from water reclamation. Desalination 301, 59–66.

Chon, K., Kim, S.J., Moon, J., Cho, J., 2012b. Combined coagulation-disk filtration process as a pretreatment of ultrafiltration and reverse osmosis membrane for wastewater reclamation: an autopsy study of a pilot plant. Water Res. 46 (6), 1803–1816.

Dubois, M., Gilles, K.A., Hamilton, J.K., Rebers, P., Smith, F., 1956. Colorimetric method for determination of sugars and related substances. Anal. Chem. 28 (3), 350–356.

Fang, K.T., Wang, Y., 1993. Number-Theoretic Methods in Statistics. CRC Press.

Federation, W.E., Association, A.P.H., 2005. Standard Methods for the Examination of Water and Wastewater. American Public Health Association (APHA), Washington, DC, USA.

Gönder, Z.B., Kaya, Y., Vergili, I., Barlas, H., 2010. Optimization of filtration conditions for CIP wastewater treatment by nanofiltration process using Taguchi approach. Sep. Purif. Technol. 70 (3), 265–273.

Her, N., Amy, G., Plottu-Pecheux, A., Yoon, Y., 2007. Identification of nanofiltration membrane foulants. Water Res. 41 (17), 3936–3947.

Jacob, M., Guigui, C., Cabassud, C., Darras, H., Lavison, G., Moulin, L., 2010. Performances of RO and NF processes for wastewater reuse: tertiary treatment after a conventional activated sludge or a membrane bioreactor. Desalination 250 (2), 833–839.

Jin, L., Zhang, G., Tian, H., 2014. Current state of sewage treatment in China. Water Res. 66, 85–98.

Lau, W.J., Ismail, A.F., 2009. Polymeric nanofiltration membranes for textile dye wastewater treatment: Preparation, performance evaluation, transport modelling, and fouling control — a review. Desalination 245 (1-3), 321–348.

Li, J., Liao, H., Normand, B., Cordier, C., Maurin, G., Foct, J., Coddet, C., 2003. Uniform design method for optimization of process parameters of plasma sprayed TiN coatings. Surf. Coat. Technol. 176 (1), 1–13.

Li, K., Wei, Y., Wang, J., Cheng, Y., Chen, M., Li, Y., 2014. Water reclamation: standards comparison and cost analysis. Acta Sci. Circumst. 34 (7), 1635–1653.

Lowry, O.H., Rosebrough, N.J., Farr, A.L., Randall, R.J., 1951. Protein measurement with the Folin phenol reagent. J. Biol. Chem. 193 (1), 265–275.

Ochando-Pulido, J., Hodaifa, G., Victor-Ortega, M., Martínez-Ferez, A., 2014. Fouling control by threshold flux measurements in the treatment of different olive mill wastewater streams by membranes-in-series process. Desalination 343, 162–168.

Shahmansouri, A., Bellona, C., 2015. Nanofiltration technology in water treatment and reuse: applications and costs. Water Sci. Technol. 71 (3), 309–319.

Stoller, M., Ochando-Pulido, J.M., 2014. About merging threshold and critical flux concepts into a single one: the boundary flux. TheScientificWorldJOURNAL 2014, 656101.

Stoller, M., Ochando-Pulido, J.M., 2015. The Boundary Flux Handbook: A Comprehensive Database of Critical and Threshold Flux Values for Membrane Practitioners. Elsevier, Amsterdam (Netherlands).

Wang, J., Wei, Y., Cheng, Y., 2013. Advanced treatment of antibiotic wastewater by nanofiltration: membrane selection and operation optimization. Desalin. Water Treat. 52 (40-42), 7575–7585.

Wang, J., Li, K., Wei, Y., Cheng, Y., Wei, D., Li, M., 2015. Performance and fate of organics in a pilot MBR-NF for treating antibiotic production wastewater with recycling NF concentrate. Chemosphere 121, 92–100.

Wintgens, T., Melin, T., Schäfer, A., Khan, S., Muston, M., Bixio, D., Thoeye, C., 2005. The role of membrane processes in municipal wastewater reclamation and reuse. Desalination 178 (1–3), 1–11.

Xu, P., Bellona, C., Drewes, J.E., 2010. Fouling of nanofiltration and reverse osmosis membranes during municipal wastewater reclamation: membrane autopsy results from pilot-scale investigations. J. Membr. Sci. 353 (1), 111–121.

Yi, L., Jiao, W., Chen, X., Chen, W., 2011. An overview of reclaimed water reuse in China. J. Environ. Sci. 23 (10), 1585–1593.